Available online at www.eccomasproceedia.org
Eccomas Proceedia COMPDYN (2017) 1606-1624

ECCOMAS
Proceedia

COMPDYN 2017
6th ECCOMAS Thematic Conference on
Computational Methods in Structural Dynamics and Earthquake Engineering
M. Papadrakakis, M. Fragiadakis (eds.)
Rhodes Island, Greece, 15–17 June 2017

EMPIRICAL UNREINFORCED MASONRY INFILL MACRO-MODEL ACCOUNTING FOR IN-PLANE/OUT-OF-PLANE INTERACTION

Mariano Di Domenico[1], **Paolo Ricci**[1], **and Gerardo M. Verderame**[1]

[1] University of Naples Federico II
Department of Structures for Engineering and Architecture
Via Claudio 21 – 80125 – Naples – Italy
{mariano.didomenico, paolo.ricci, verderam}@unina.it

Keywords: URM infill wall, out-of-plane, empirical, database, in-plane/out-of-plane interaction, macro-model.

Abstract. *Unreinforced Masonry (URM) infills are widely used in Reinforced Concrete (RC) structures in Mediterranean countries. URM infills are subjected to the seismic action in their plane, i.e. in the In Plane (IP) direction, and in the Out Of Plane (OOP) direction. The IP displacement demand reduce the OOP capacity and vice-versa: this phenomenon is called IP-OOP interaction. A large number of studies has been carried out on the IP behaviour of infills, while their OOP response and the IP-OOP interaction have been less investigated. In this paper, a review of code and literature provisions concerning URM infills OOP behaviour is presented together with a review of the experimental tests carried out to investigate the infills OOP response and the effects of the IP-OOP interaction. An experimental database is collected to assess the effectiveness of literature and code provisions and to propose new empirical formulations both for predicting infills OOP strength, stiffness and displacement capacity and for modelling the effects of IP displacement demand on the OOP behavior and vice versa. A state of art on infills OOP behaviour and IP-OOP interaction modelling is presented. Most of these distributed-plasticity models are not based on experimental evidences and do not allow taking into account the IP and OOP stiffness degradation due to OOP and IP actions, respectively. A lumped-plasticity macro-model based on the proposed empirical formulations and conceived to represent the IP and the OOP behavior taking into account the mutual interaction effects is defined. Part of the proposed modelling strategy is a routine that removes the whole infill panel from the structural model in case of its IP or OOP collapse. The proposed model is used for an example application showing the effects of taking into account or neglecting the IP-OOP interaction phenomena during structural analyses.*

Peer-review under responsibility of the organizing committee of COMPDYN 2017.
doi: 10.7712/120117.5516.17533

1 INTRODUCTION

It is well—known from past and recent earthquakes that damaging of exterior partitions in Reinforced Concrete (RC) buildings, such as Unreinforced Masonry (URM) infill walls, may cause important functional and financial losses (e.g., [1-4]) among many others), especially in existing RC buildings, which were not designed by applying provisions aimed at damage limitation. Moreover, infill collapse may represent a serious risk for life safety [5]. An URM infill is generally excited by in-plane (IP) seismic action, which is the main cause of infills damaging. A very large number of experimental tests and modelling proposals concerning infills' IP behaviour are proposed in literature, e.g. in [6-10], among many others. Moreover, infills are subjected to Out-Of-Plane (OOP) seismic accelerations, which may provoke the collapse with overturning from the structural frame. IP damaging could favour the OOP collapse of infills by reducing their OOP stiffness, strength and displacement capacity. This phenomenon is called IP-OOP interaction.

In this work, a review of URM infills' OOP capacity models proposed in literature and adopted by technical codes aimed at testing their predicting capacity on the results of pure OOP and IP-OOP tests, which are briefly described, is reported. Empirical formulations aimed at predicting the OOP first macro-cracking load, strength and displacement capacity of URM infills are proposed, in order to define a trilinear OOP backbone in a semi-empirical framework. Based on experimental tests' results, relationships aimed at modelling the OOP stiffness, strength and displacement capacity reduction due to IP damaging and vice-versa are proposed. Based on these formulations, a new infill macro-model accounting for IP-OOP interaction is proposed and applied through Incremental Dynamic Analyses on a simple example frame, in order to show the effects of IP-OOP interaction in the seismic capacity assessment of RC frames.

2 STATE-OF-THE-ART

Literature and code provisions concerning the OOP behaviour modelling of URM infills are herein described, together with a brief recall of experimental tests aimed at assessing their pure OOP behaviour and the IP-OOP interaction effects. A detailed state of the art on OOP infills strength can be found in [11].

2.1 OOP behaviour of infills in literature

A closed-form solution for the prediction of the lateral stiffness of an isotropic elastic plate was proposed by Timoshenko in [12]. This relationship could be eventually used to predict URM infills initial stiffness: in fact, an infill panel loaded in the OOP direction behaves like an orthotropic elastic plate up to first cracking. After first cracking, the strength against external OOP loads is attributed to a resistant mechanism called "arching action", first individuated by McDowell [13]. Neglecting the arching action, the OOP strength is determined at the attainment of the masonry tensile strength at the outermost fiber in tension. For an infill considered as an elastic plate, it can be computed through Timoshenko's formula proposed in [12]. Clearly, such an approach produces a prediction more similar to a first cracking load. In literature, several relationships that consider arching action are proposed, such as McDowell's expression [13], Angel et al.'s formulation [14], Dawe and Seah's formulation proposed in [15], Klinger's analytical relationship given in [16]. In [17], indirectly, Abrams proposes a relationship to compute the displacement of an infill at peak load. This formulation was modified by Flanagan and Bennett in [18], together with Dawe and Seah's expression for peak load. Kadysiewski and Mosalam [19] compute infills OOP secant stiffness at peak load through a method based on the first OOP natural frequency of distributed-mass beams considered

pinned at ends proposed by Blevins in [20]. After the attainment of the peak load point, the panel undergoes a severe and extended damage that causes a progressive reduction of its load bearing capacity. For this reason, generally, after peak load, in the OOP force-displacement relationship a softening branch is expected. Due to stresses redistribution, the post-peak behaviour could even be plastic. Note that a conventional definition of OOP collapse displacement is not available. In [19] Kadysiewski and Mosalam assume the displacement capacity of infills equal to 5 times the panel displacement at peak load. Several authors observe that the ultimate displacement of infills should not exceed the panel thickness [19, 21, 22].

2.2 OOP behaviour of infills in code provisions

FEMA273 [23], in section 7.5.3.1, lists the conditions that allow considering arching action in the assessment of infills OOP strength, such as the effectiveness of the infill connection to the surrounding frame, its columns and beams stiffness and strength, and the panel slenderness. As pointed out in FEMA274 [24], FEMA273 compute URM infills OOP strength through a conservative simplification of Angel et al.'s formula, which is instead proposed in its original formulation by FEMA306 [25] and NZSEE2006 [26]. Eurocode 6 [27], in section §6.3.2, proposes an expression to calculate the lateral strength of masonry walls based on arching action; this relationship can be extended, potentially, to URM infills. FEMA 273 (section 7.5.3.3) and FEMA 356 [28] (section 7.5.3.3) provide some indications concerning displacement capacity of URM infills, expressed as a percentage of the panel's height, at different Limit States. FEMA 273, 306 and 356 suggest to use Angel et al.'s formulation, in its original or simplified form, to evaluate the OOP strength of URM infills and propose the use of Abrams' formulation [18] to calculate the OOP displacement at peak load. This is an implicit way to define URM infills' stiffness at peak load.

2.3 Experimental tests

Experimental pseudo-static tests aimed at characterizing the OOP behaviour of URM infill wall panels and the effects of IP/OOP interaction were performed by different authors on full- or reduced-scale specimens.

Pure OOP tests were carried out on concrete hollow bricks infills in steel frames by Dawe and Seah [15]. Griffith and Vaculik [29] tested URM clay hollow bricks infills pinned or clamped at edges in different configurations. IP-OOP interaction is usually investigated through IP cyclic tests followed, at the infill IP unloading, by OOP monotonic tests. Such tests were performed by Flanagan and Bennett [30, 31], Angel et al. [14], Calvi and Bolognini [32], Pereira et al. [33], Guidi et al. [34], Furtado et al. [35, 36] and Hak et al. [37]. These authors investigated the effects on IP/OOP interaction of different parameters, such as infills' slenderness, aspect ratio, loading conditions. In [30, 31], Flanagan and Bennett also present the results of a IP tests carried out after OOP loading. Some characteristics of the experimental tests above described are reported in Table 1.

Authors		test type	frame type	load type*	infill type**	h [m]	w [m]	t [mm]	h/t
Dawe and Seah	[15]	OOP	Steel	U	CoHB	2.80	3.60	90-190	14.7-31
Griffith and Vaculik	[29]	OOP	absent	U	CHB	2.50	2.50-4.00	110	22.7
Angel et al.	[14]	IP+OOP	R.C.	U	CB/ CMU	1.625	2.44	48-190	9-34
Flanagan and Bennett	[30, 31]	IP+OOP	Steel	U	CHB	2.24	2.24	100-330	6.8-22.4
Calvi and Bolognini	[32]	IP+OOP	R.C.	C	CHB	2.65	4.20	135	19.6
Pereira et al.	[33]	IP+OOP	R.C.	U	CHB	1.70	3.50	150	11.3
Guidi et al.	[34]	IP+OOP	R.C.	C	CHB	2.65	4.15	120-300	8.8-22.1
Furtado et al.	[35, 36]	IP+OOP	R.C.	U	CHB	2.30	4.20	150	15.3
Hak et al.	[37]	IP+OOP	R.C.	C	CHB	2.95	4.22	350	8.4

* U: Uniformly distributed, L: Linear, C: Concentrated.

** C: Clay, Co: Concrete, H: Hollow, B: Bricks, CMU: Concrete masonry units.

Table 1. Specimens characteristics available in the literature.

3 ASSESSMENT OF LITERATURE AND CODE PROVISION

The analysis of tests recalled in the previous section allowed the collection of experimental values of URM infills OOP force, secant stiffness and displacements at first macro-cracking and peak load. Maximum displacements attained during tests were also collected. With reference to single-wythe infills restrained on four edges in a confining frame, the collected data are reported in Figures 1 and 2.

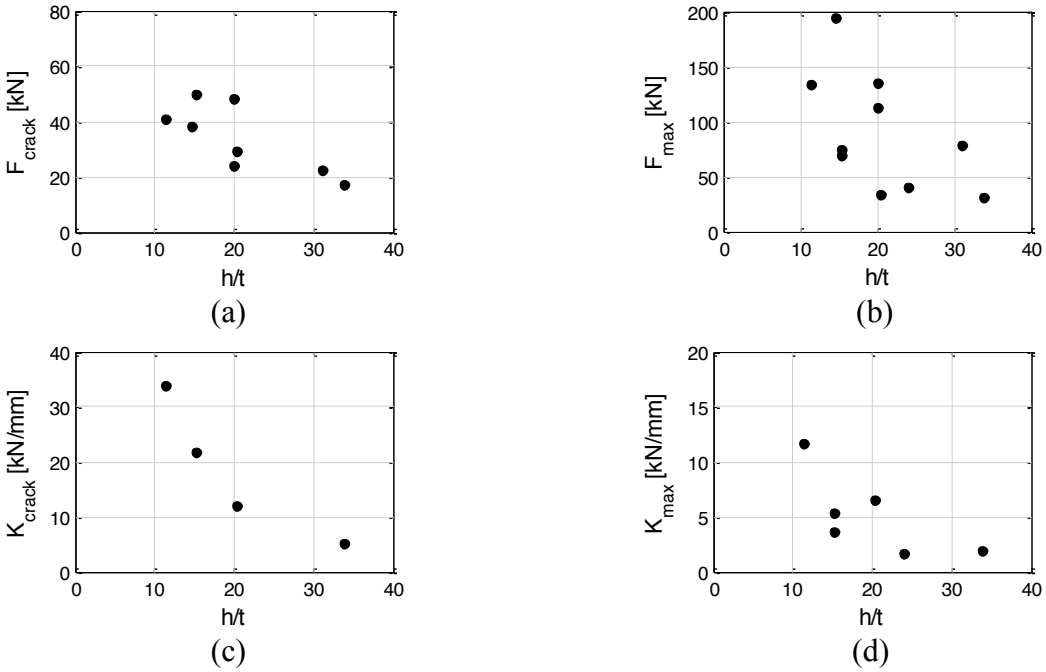

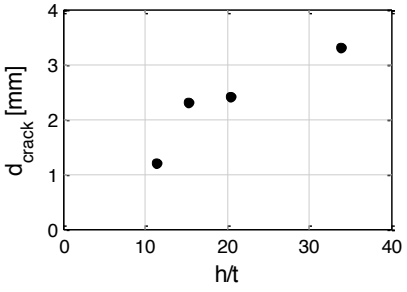

(e)

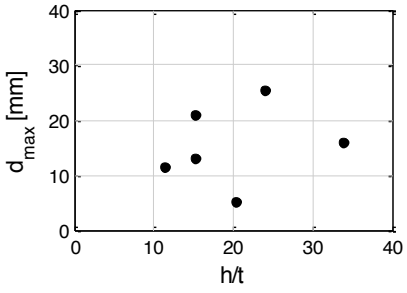

(f)

Figure 1. Experimental data collected: Fcrack (a), Kcrack (b), dcrack (c), Fmax (d), Kmax (e), dmax (f) vs the tested panels slenderness.

Mean, median and CoV of the experimental-to-predicted ratios for the collected parameters and the considered literature formulations are reported in Table 2a and 2b.

	F_{crack}	K_{crack}	K_{max}	d_{max}		d_u		
Author/ Code	**Timoshenko [12]**		**K&M [19]**	**Abrams [17]**	**Abrams+ F&B [18]**	**FEMA-LS [23]**	**FEMA-CP [23]**	**K&M [19]**
mean	47.07	0.99	1.02	0.33	0.34	0.50	0.30	3.94
median	19.99	0.91	0.82	0.37	0.39	0.38	0.23	1.21
CoV [%]	90	50	61	59	71	76	76	107

Table 2a. Mean, median and CoV of the experimental to predicted ratios for characteristic forces, stiffnesses and displacements.

	Code provisions			**Literature proposals**				
Author/ Code	**FEMA 273 [23]**	**FEMA 356 [28]**	**EC6 [27]**	**McDowell [13]**	**Angel [14]**	**D&S [15]**	**D&S+ F&B [18]**	**Klinger [16]**
mean	5.37	4.36	1.09	0.64	1.82	1.33	1.46	0.65
median	3.80	3.08	0.73	0.43	1.45	1.07	1.17	0.31
CoV [%]	97	97	111	111	79	70	70	121

Table 2b. Mean, median and CoV of the experimental to predicted ratios for Fmax.

Timoshenko's first micro-cracking load is, as expected, low with respect to the considered first macro-cracking loads, while the elastic stiffness of the plate predicted by Timoshenko results in good agreement with the secant stiffness at first macro-cracking, despite an expected little overestimation.

Dawe and Seah's formulation [15], which accounts for double arching action, is the best-predicting model for OOP strength, while Kadysiewski and Mosalam's [19] approach produces a good, even if underestimating, prediction of the secant stiffness at the same point. The underestimation is expected considering that Kadysiewski and Mosalam's prediction is based on the behaviour of a mass-distributed beam and does not account for the infill plate behaviour. d_{max} seems to be unpredictable through the application of literature and code recommendations.

Only Flanagan and Bennett [30, 31], Calvi and Bolognini [32] and Furtado et al. [35, 36] state that their tests were performed until the OOP infill collapse, even if this condition, and

so the corresponding "collapse displacement", is not conventionally defined. The few collected data are reported in Figure 3. As shown in Table 2a, the 3% of the panel height seems to be an overestimation of the panel ultimate displacement, which is underestimated, instead, by Kadysiewski and Mosalam's modelling approach.

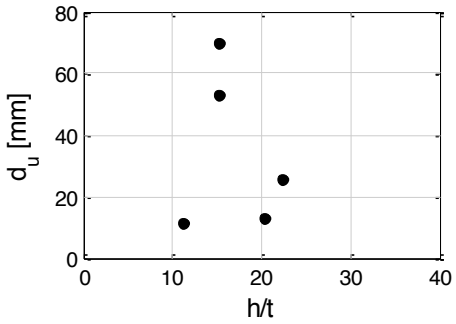

Figure 2. Experimental ultimate displacements vs the tested panels slenderness.

4 SEMI-EMPIRICAL PREDICTION OF URM INFILLS OOP BEHAVIOUR

A semi-empiric approach is hereafter proposed in order to define the characteristic points of a tri-linear OOP response backbone based on geometric and mechanical properties of infills. Note that, in the following relationships, lengths are expressed in meters and stresses are expressed in megapascals. The empirical relationships proposed herein were defined by correlating the observed values of strength and stiffness with five geometric and mechanical properties of infills (t, h, w, f_m', E) through a linear least-square regression. Among these, the significant parameters retained in the proposed relationships were determined through F-tests on the null-hypothesis of statistical equivalence of the model containing all parameters and all possible model retaining less than five predictive parameters [38]. The retained parameters in the proposed models are the same parameters included all mechanical-based model accounting for vertical arching (such as Angel et al.'s, McDowell's, Eurocode's capacity models). The contribution to q_{crack} and q_{max} increase or decrease of the retained predictive parameters are simply explainable with reference to basic mechanical principles applied to an equivalent elastic beam in which arching action occurs. The above-described regressions provided Equation (1), which produces experimental-to-predicted ratios with mean 1.02, median 1.04, CoV 20%, and Equation (2), which produces experimental-to-predicted ratios with mean 1.01, median 1.00, CoV 18%:

$$q_{crack} = 0.31 \; f_m'^{\,0.05} \frac{t}{h^{2.66}} \tag{1}$$

$$q_{max} = 1.95 \; f_m'^{\,0.35} \frac{t^{1.59}}{h^{2.96}} \tag{2}$$

Clearly, F_{crack} and F_{max} (see Table 3) are obtained by multiplying q_{crack} and q_{max} for the area of the infill panel.

Due to the little number of available experimental data, potential overfitting issues prevent the definition by regression of empirical relationships for K_{crack}, K_{max} and d_u prediction. Based on the results of the comparison of Timoshenko's [12] and Kadysiewski and Mosalam's [19] models' predictions with experimental data, it is recommended to use those relationships to define first cracking point and peak load stiffnesses. To predict d_u an "empirical" value of the

infills OOP ductility, equal to 3.7, has been calculated through the mean value of the ratio of the observed ultimate displacement discussed in section 2.1 over the displacement at peak load obtained by dividing the results of Equation 2 and Kadysiewski and Mosalam's stiffness.

In Table 3 the mean, median and CoV of experimental-to-predicted ratios for all considered capacity parameters are reported, with reference to a possible model based on literature proposals or on semi-empirical formulations.

		Literature-based approach			**Semi-empirical approach**		
First cracking point	**F_{crack}**				Eq. 1	*mean*	1.02
						median	1.04
						CoV [%]	20
	K_{crack}				Timoshenko [12]	*mean*	0.99
						median	0.91
						CoV [%]	50
	d_{crack}				F_{crack}/K_{crack}	*mean*	0.83
						median	0.77
						CoV [%]	15
Peak load point	**F_{max}**	Dawe and Seah [15]	*mean*	1.33	Eq. 2	*mean*	1.01
			median	1.07		*median*	1.00
			CoV [%]	70		*CoV [%]*	18
	K_{max}	Kadysiewski and Mosalam [19]	*mean*	1.02	Kadysiewski and Mosalam [19]	*mean*	1.02
			median	0.82		*median*	0.82
			CoV [%]	61		*CoV [%]*	61
	d_{max}	F_{max}/K_{max}	*mean*	1.30	F_{max}/K_{max}	*mean*	1.14
			median	0.82		*median*	1.20
			CoV [%]	91		*CoV [%]*	57
Collapse	**d_u**	FEMA 273 [23]	*mean*	0.50	$d_u=\mu d_{max}$	*mean*	1.00
			median	0.38		*median*	0.75
			CoV [%]	76		*CoV [%]*	70

Table 3. Literature-based and semi-empirical modelling proposals.

5 OOP BEHAVIOUR AT GIVEN IP DAMAGE

IP+OOP tests by Flanagan and Bennett, [30, 31], Angel et al., [14], Calvi and Bolognini, [32], Furtado et al., [35, 36], Hak et al., [37], allowed assessing the degradation of force and stiffness at first cracking and peak load. To prevent overfitting due to the little number of data, it is assumed that the stiffness and strength degradation are related only to the IP IDR demand normalized with respect to the IDR at IP collapse, IDR_u. The obtained relationships have a structure of this type:

$$\frac{P_{dam}}{P_{undam}} = \begin{cases} \min\left\{1\,;\,\alpha\left(\frac{IDR}{IDR_u}\right)^{\beta}\right\} & \text{if } IDR < IDR_u \\ 0 & \text{if } IDR \geq IDR_u \end{cases} \quad (3)$$

in which P_{dam} is the observed variable for the infill that underwent a maximum IP displacement represented by the IDR, P_{undam} is the observed variable for the undamaged infill, and the α and β coefficients are determined through a linear least squares regression in the log-log

space. Clearly, P_{dam}/P_{undam} cannot be higher than 1 and must be equal to 0 if $IDR \geq IDR_u$, i.e., the OOP capacity drops to zero at the infill IP collapse. If IP tests were stopped prior to the complete infill's resistance loss, IDR_u was calculated by applying Fardis and Panagiotakos [6] proposal.

In Figure 3 the experimental degradation data as a function of IDR/IDR_u, as well as α and β values, are shown. Moreover, by applying the proposed relationships to predict the degradation ratio for the tested panels, the mean, median and the CoV of the experimental-to-predicted degradation ratios for each OOP capacity parameter are shown.

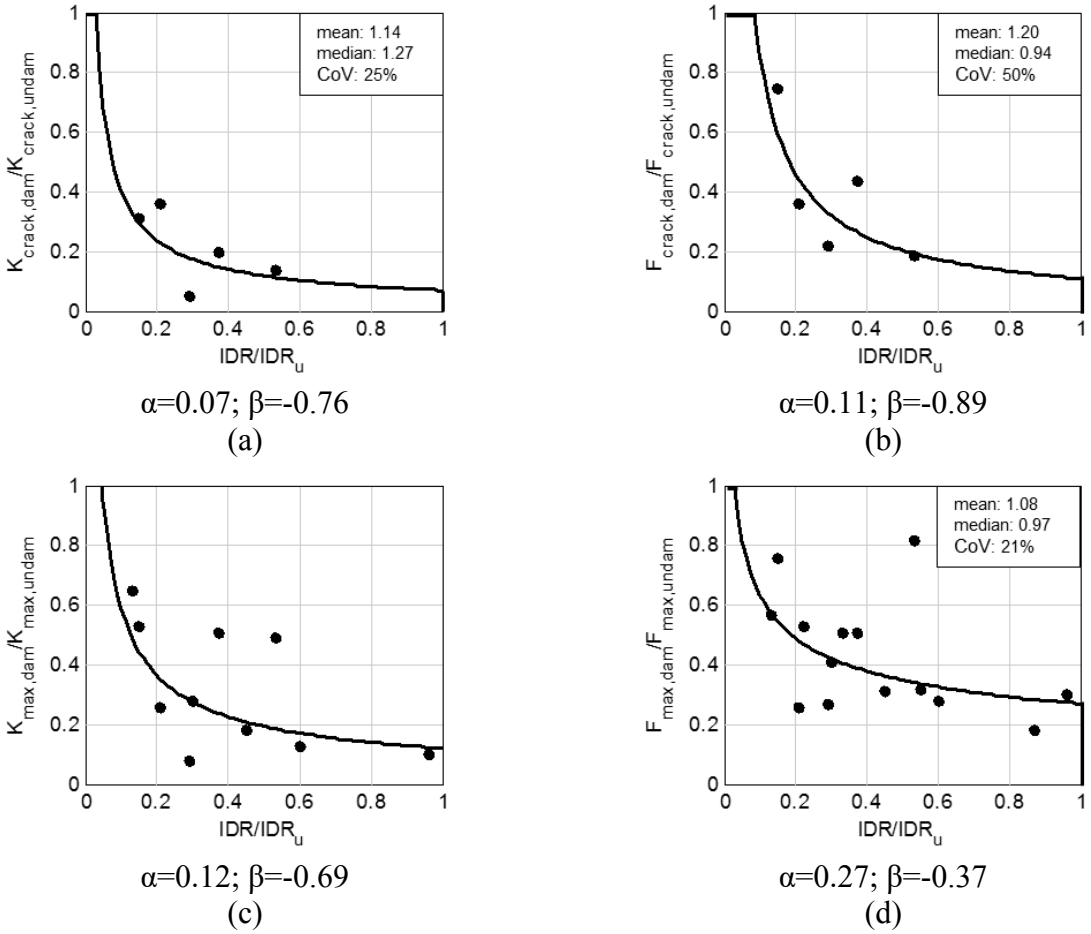

Figure 3. Experimental data collected: Kcrack,dam/Kcrack,undam (a), Fcrack,dam/Fcrack,undam (b), Kmax,dam/Kmax,undam (c), Fmax,dam/Fmax,undam (d) vs the tested panels IDR/IDR_u ratios. Mean, median and CoV of the experimental-to-predicted ratios.

To model the peak load degradation of thick and strong URM infills, also Hak et al.'s [37] points were introduced in the database. In this case, the OOP resistance of the undamaged panel is set equal the OOP peak load force predicted through the empirical relationship presented in this study (Eq. 2).

OOP first cracking and peak load displacements of IP damaged infills are determined through the ratios of the corresponding degraded forces and stiffnesses.

5.1 OOP ultimate displacement given an IP damage

Furtado et al. [35, 36] showed that at an IDR equal to 0.5%, the $d_{u,dam}/d_{u,undam}$ ratio resulted equal to 0.7 for Inf_03. Based on Panagiotakos and Fardis model, Inf_03 attains a complete IP

resistance loss for IDR=2.38%, which is assumed as IDR_u. This means that, accordingly to Furtado et al.'s result, for $IDR/IDR_u=0.21$, $d_{u,dam}/d_{u,undam}=0.7$. This is the only reliable datum concerning the OOP displacement capacity reduction due to IP damage available in literature. In this work it is assumed that the $d_{u,dam}/d_{u,undam}$ ratio is equal to 1 for IDR=0 and to 0 for $IDR=IDR_u$: a linear trend between these two points seems to be an acceptable assumption (Equation 4) with respect to the position of Furtado et al.'s point shown in Figure 4. Note that this approach is consistent with the proposal of Fardis in section 3.5 of [39].

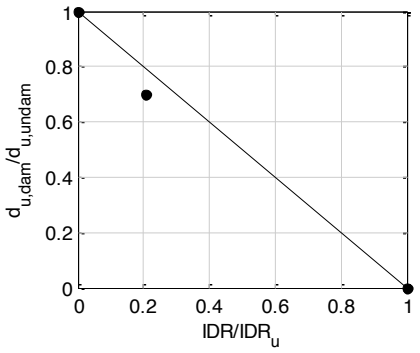

$$\frac{d_{u,dam}}{d_{u,undam}} = 1 - \frac{IDR}{IDR_u} \tag{4}$$

Figure 4. OOP ultimate displacement reduction due to the IP demand represented by the ratio of the current IDR over the collapse IDR based on Furtado's [35, 36] experimental datum.

5.2 OOP backbones at given IP damage

Based on the above discussed issues, the backbone of the OOP behaviour of the undamaged panel varies due to IP displacements as shown in the example Figure 5 for various IDR levels.

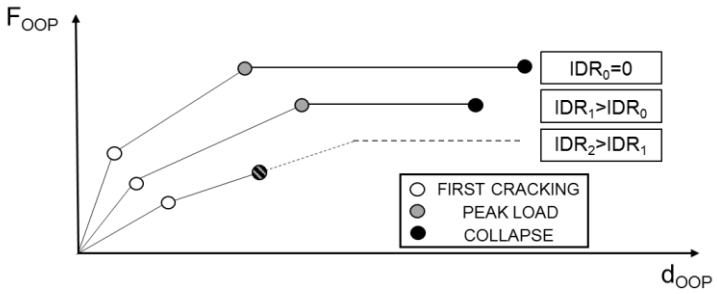

Figure 5. Example OOP backbones for IP undamaged and damaged infills.

If, for high values of the IDR, the predicted collapse OOP displacement becomes smaller than the predicted displacement at peak load, a brittle OOP failure is considered, without ductility. In Figure 6, the experimental and predicted OOP diagrams are shown for some IP undamaged and damaged panels. The characteristic points of the predicted behaviour diagram are determined by using the semi-empirical approach herein proposed.

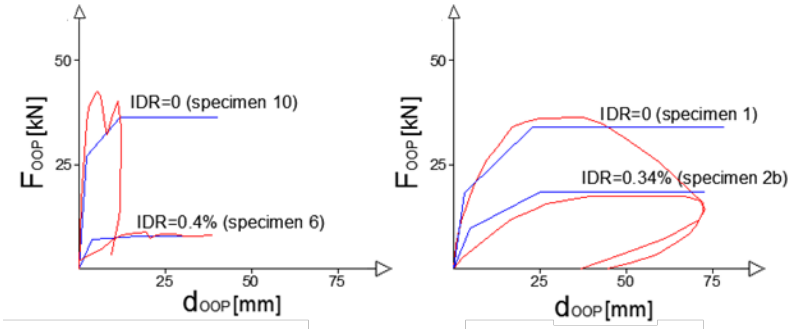

Figure 6. A comparison of experimental and predicted OOP behaviour diagrams for (a) specimens 10 and 6 by Calvi and Bolognini, (b) specimens 1 and 2b by Angel et al.

6 IP BEHAVIOUR AT GIVEN OOP DAMAGE

The effects of OOP damage on the IP behaviour of infills have been less studied than the vice-versa, especially in terms of experimental tests. Flanagan and Bennett, in [30], applied a "combined" IP/OOP loading on specimen 23. The procedure consisted in alternatively apply IP/OOP loads at fixed OOP/IP displacements. During each OOP tests, it was observed that the IP load that allowed keeping constant the fixed IP displacement decreased. The reconstructed IP force-displacement relationship for specimen 23 is shown in Figure 7. The obtained IP backbone can be compared to the one defined for the control specimen 2, which was identical to specimen 23 and was tested only IP up to collapse.

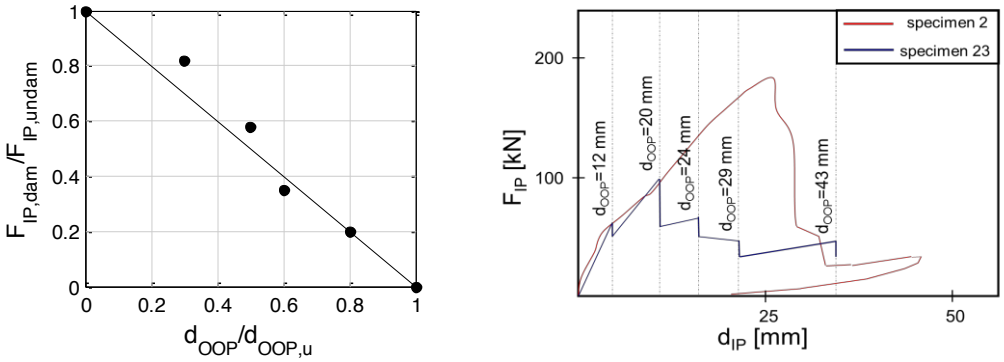

Figure 7. Extrapolated IP force degradation based on Flanagan and Bennett's specimens 2 and 23 behaviour (a) shown in (b).

In Figure 7b, for each drop of the IP load at fixed IP displacement, the maximum OOP displacement attained during the OOP test that produced that drop is indicated. IP displacements at which the IP tests were stopped are associated:

1) to the maximum OOP displacement attained during the corresponding OOP test normalized with respect to the undamaged infill OOP collapse displacement;
2) to the ratio of the corresponding force on the specimen 23 reconstructed IP backbone over the force on the specimen 2 IP backbone.

So, through the IP displacement, the ratios defined in the above points 1) and 2) are related in Figure 7a. Note that in this Figure, the point corresponding to d_{OOP}=43 mm in Figure 7b

was dropped, given that that OOP displacement was greater than the OOP ultimate displacement evaluated for the undamaged panel (specimen 18).

For this reason, at the attainment of an OOP maximum displacement d_{OOP}, the IP force that produces the IP displacement d_{IP}, $F_{IP,dam}(d_{IP}, d_{OOP})$ can be expressed through a simplified linear relationship as:

$$\frac{F_{IP,dam}(d_{IP}, d_{OOP})}{F_{IP,undam}(d_{IP})} = 1 - \frac{d_{OOP}}{d_{OOP,u}} \tag{5}$$

in which $F_{IP,undam}(d_{IP})$ is the IP force that produces the IP displacement d_{IP} of the undamaged panel and $d_{OOP,u}$ is the undamaged infill OOP collapse displacement.

Experimental data concerning the IP collapse displacement reduction due to OOP actions are not available.

7 PROPOSED MODELLING STRATEGY

Hashemi and Mosalam [41] and Kadysiewski and Mosalam [19] proposed modelling strategies of infills OOP behaviour and IP + OOP interaction based on the results of FEM analyses. Furtado et al., [42], Longo et al., [43], Shing et al., [44], proposed improvements of Kadysiewski and Mosalam's model. A distributed-plasticity infill model was proposed by Oliaee and Magenes in [45]. In this section, a new macro-model for infill walls is presented. The proposed model has been implemented in OpenSEES [46] and has been conceived to model infills' IP and OOP behaviour by applying whichever material model or hysteretic rule and accounting for both OOP/IP strength and stiffness degradation due to IP/OOP interaction, in order to assess the seismic capacity of infills and the seismic demand acting on them correctly.

First, the OOP behaviour of the undamaged infill should be defined. For instance, an OOP trilinear backbone can be defined through the semi-empirical approach described in section 5 (IDR=0 backbone). Then, n IDR_i (with $i=1, ..., n$) backbones should be defined through the degradation-modelling relationships proposed in section 5. Each one of these curves describes the OOP behaviour that the infill will exhibit once the IP IDR demand exceeds the threshold set by IDR_i (see Figure 8).

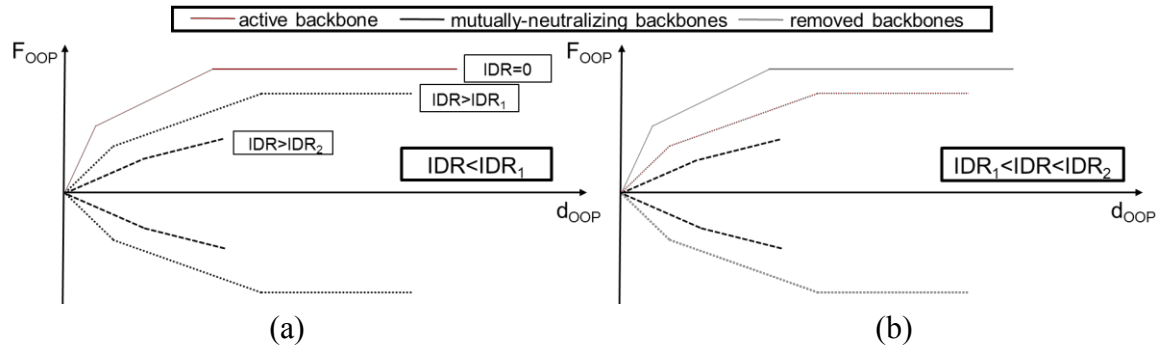

Figure 8. Proposed modelling strategy of the IP/OOP interaction. Active and mutually-neutralizing OOP backbones for $IDR<IDR_1$ (a); active, mutually-neutralizing and removed backbones for IDR between IDR_1 and IDR_2 (b).

As shown in Figure 9, A diagonal element is used to model the infill. The diagonal element is pinned at ends and is provided of a central node connected to a second central node in

which the mass participating to the first OOP vibration mode of the infill is lumped: generally, it can be assumed equal to the 81% of the panel total mass [19].

2n+1 plastic hinges, i.e., in OpenSEES, 2n+1 ZeroLength Elements, are used to connect the two central nodes. First, a plastic hinge defined through the IDR=0 backbone must be implemented. Then, for each IDR=IDR_i backbone, a couple of plastic hinges must be defined: an "i-th real plastic hinge", modelling carrying the IDR_i backbone and an "i-th auxiliary plastic hinge", carrying the IDR=IDR_i backbone mirrored with respect to the displacements axis. This means that the OOP force for a given OOP displacement in the i-th real plastic hinge is always equal and opposite to the OOP force at the same displacement in the i-th auxiliary plastic hinge. This also means that as long as all plastic hinges are part of the infill model, the panel OOP behaviour is the one defined by the IDR=0 backbone, while the effects of the other plastic hinges are mutually neutralizing.

In the following example, an Hysteretic Material is used to model real plastic hinges and a Parallel Material with scale factor equal to -1 is used to model auxiliary plastic hinges. Nevertheless, the proposed modelling strategy allows the user to model the IP and OOP infills behaviour (both non-degraded and degraded) with any desired trilinear material model as well as with any hysteretic rule.

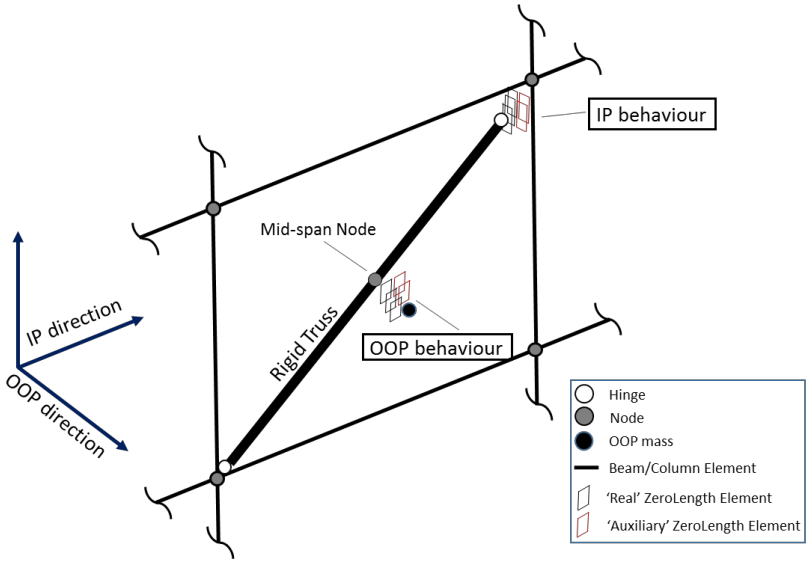

Figure 9. Graphical representation of the proposed modelling strategy.

A routine that removes from the structural model the IDR_{i-1} real plastic hinge and the IDR_i auxiliary plastic hinge when the IP IDR_i is implemented. In this way, as soon as the IDR exceeds IDR_i and as long as the IDR is lower than the successive IP damage threshold IDR_{i+1}, the panel OOP behaviour is defined by the IDR=IDR_i backbone "contained" in the i-th real plastic hinge, while the effects of the remaining plastic hinges are still mutually neutralizing. Moreover, if the OOP displacement exceeds the ultimate displacement associated to the IDR=IDR_i backbone, all the elements representative of the infill wall are removed from the structural model.

In a totally identical way, the IP strength and stiffness degradation, as well as the whole infill collapse and removal from the structural model due to the attainment of the IP collapse displacement, can modelled and controlled through the ratio between the OOP displacement demand and the OOP displacement capacity of the undamaged panel.

7.1 Application on a case-study RC frame

The proposed model is herein applied to model a one-leaf URM infill, with thickness equal to 100 mm, of a simple one-bay one-storey RC frame. OpenSEES code has been used to carry out Incremental Dynamic Analyses (IDAs) [47] on a model accounting for IP/OOP interaction (W/ Model) and on a model in which the interaction was not active (W/O model).

The case-study frame was designed according to Eurocode 2 [48] and Eurocode 8 dispositions. A C28/35 concrete and a reinforcement steel with yield strength equal to 450 N/mm^2 were used. The longitudinal reinforcement in the beam was defined by applying the minimum percentage allowed by EC2, while shear-flexure and beam-column capacity design rules were applied to define the beam transverse reinforcement and the column reinforcement. The mechanical properties assigned to the infill masonry are obtained by wallette tests reported in [39]. The characteristics of the example infilled frame are shown in Table 4.

	Element Length	**Cross Section**	**Longitudinal bars**	**Stirrups at ends**
Columns	3200 mm	300×400 mm^2	8ϕ18	ϕ8@50 mm
Beam	4000 mm	300×400 mm^2	3ϕ14 (top and bot.)	ϕ8@75 mm
	height	**width**	**thickness**	
Infill Wall	2800 mm	3600 mm	100 mm	
Masonry mechanical properties				
$\mathbf{f'_m}$	2.4	N/mm^2	in the vertical direction	
$\mathbf{E_m}$	2500	N/mm^2		
$\boldsymbol{\tau_{cr}}$	0.3	N/mm^2		

Table 4. Geometric and mechanical properties of the example infilled RC frame.

An Eurocode-based approach [49] was used to model structural non-linearity. For instance, an elastic-perfectly-plastic with cracking point backbone was used to model RC members non-linear behaviour. The infill IP behaviour was modelled according to Panagiotakos and Fardis [7], with the slope of the softening branch assumed equal to -2% of the slope of the initial elastic branch. The infill OOP behaviour was modelled through the semi-empirical approach introduced in section 5. The IDR_u predicted through Panagiotakos and Fardis' approach was 2.2%, while the OOP collapse displacement for the undamaged panel predicted by the proposed empirical approach was $d_{OOP,u}$=89 mm. The infill wall behaviour degradation was modelled through the proposed empirical-based approach: for instance, the IP and OOP degradation was modelled with backbones defined at steps of 0.05 times the $d_{OOP,u}$ displacement and the IDR_u, respectively. The IP and OOP "real" backbones are shown in Figure 12. The example frame is provided of a lumped mass active in the IP direction equal to 25000 kg, while a mass active in the OOP direction equal to 665 kg is lumped in the center of the element, representative of the mass participating to the first OOP vibration mode of infill wall, as above described. The frame was subjected to the 22 bidirectional ground motions of the ATC-63 Far-field Ground Motion Set [50]. For each ground motion, the first component was applied in the IP direction, while the second one was applied in the OOP direction. The analyses were carried out by applying mass- and tangent stiffness-proportional Rayleigh damping rules and assigning a damping ratio equal to 2% for the IP vibration mode. A damping ratio equal to 2% was also assigned to the OOP vibration mode: this choice is due to the lack of exhaustive studies on this topic, which is worth to be investigated in the future. The IDA curves for all records and for W/ and W/O Models are shown in Figure 10 together with median IDA

curves. As expected, the predicted displacement demands for W/ Model are greater than the ones registered for W/O Model.

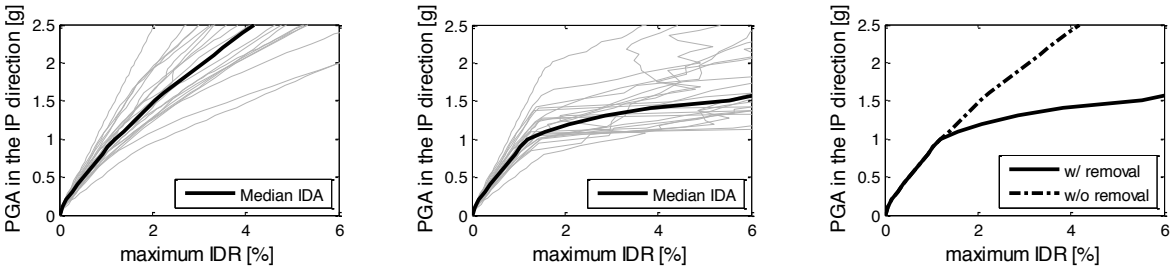

Figure 10. IDA curves for W/O (a), W/ (b) models with median IDA curves for both models (c).

Now, let us consider a specific ground motion (Ground Motion 14 of the ATC-63 set) and the corresponding IDA curves obtained for W/ and W/O Models (Figure 11).

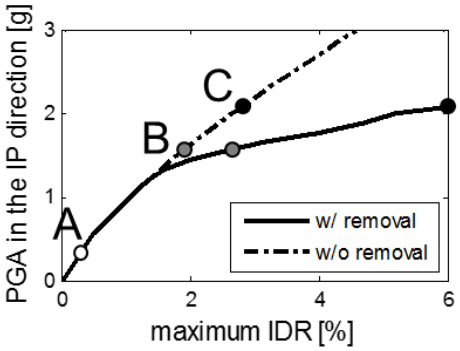

Figure 11. IDA curves for Ground Motion 14.

At "check point" A, for a PGA in the IP direction equal to 0.30 g, the displacement demands in both the IP and the OOP direction caused no interaction phenomena: no backbone was removed, as shown in Figure 12, and the displacement time-histories in the IP direction for the two models do not differ from each other.

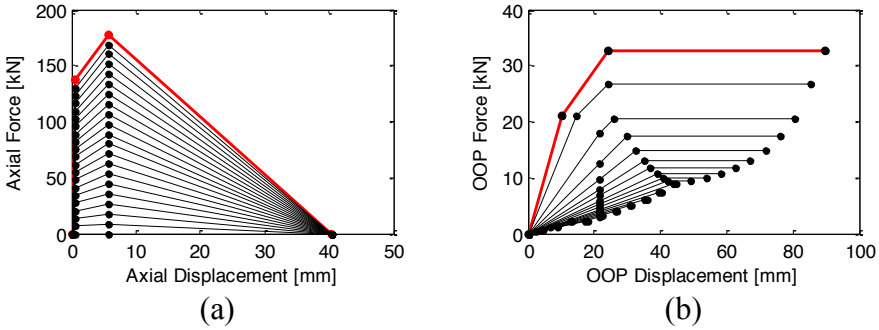

Figure 12. IP (a) and OOP (b) active (red) and mutually-neutralizing (black) backbones at the end of Check Point A analysis. Note that the IP backbones are referred to the axial behaviour of the diagonal element representative of the infill wall.

At "check point" B, for a PGA in the IP direction equal to 1.60 g, the displacement demands in both the IP both the OOP direction produced the infill's strength and stiffness degradation, as shown in Figure 13, but not the infill collapse and removal from the structural model.

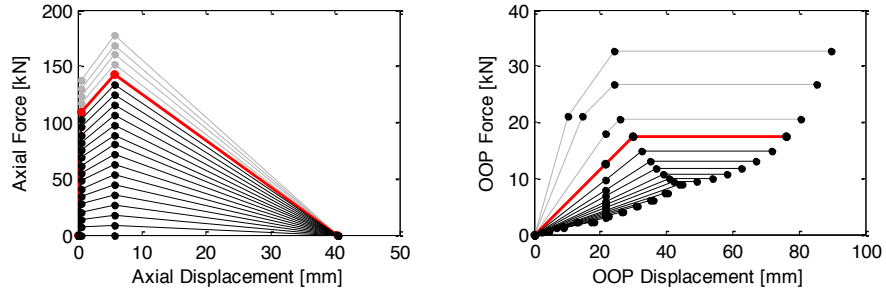

Figure 13. IP (a) and OOP (b) removed (grey), active (red) and mutually-neutralizing (black) backbones at the end of Check Point B analysis.

The IP degradation produced a perceptible variation in the maximum IP displacement attained by the example frame as well as in the whole IP displacement time history. The maximum IDR demand passed from about 1.8% for W/O Model to about 2.7% for W/ Model.
At "check point" C, for a PGA in the IP direction equal to 2.10 g, the displacement demands in both the IP and the OOP direction produced the infill's strength and stiffness degradation and then the infill collapse and removal from the structural model. The infill removal produced a significant variation in the IP displacement time history: the maximum IDR demand passed from about 2.9% for W/O Model to about 5.9% for W/ Model. This outcome points out the importance of infills' degradation and collapse modelling in order to correctly estimate the seismic capacity of infilled structures at collapse condition.

8 CONCLUSIONS

This work is focused on the OOP behaviour of URM infills and on the effects of IP damage on it and vice-versa, i.e., on the IP/OOP interaction.

First, literature analytical and empirical models for the prediction of the OOP stiffness and force at first macro-cracking and peak load, together with predicting models for the OOP collapse displacements were considered. Some of these capacity models were adopted, in a simplified form, by technical codes. So, code and literature provisions were applied on experimental tests' result to assess their effectiveness. This comparison has shown that literature provides quite good models for the prediction of the initial and secant at peak load stiffnesses of URM infills, as well as of their OOP strength. No literature nor code model produces predictions in good agreement with the experimental values of first macro-cracking load and OOP collapse displacement. Experimental data were used to carry out linear least squares regressions to obtain empirical formulations aimed at predicting the OOP first macro-cracking load, the OOP collapse displacement and to obtain an empirical formulation which improves the capacity to predict URM infills OOP strength. A trilinear backbone for URM infills was so defined in an empirical-based framework. Empirical relationships aimed at modelling the OOP behaviour modifications due to IP damaging and vice-versa were also defined. A new macro-modelling strategy based on the proposed empirical relationships is presented. Details on the model implementation in OpenSEES are reported. The proposed model is applied on a case-study one-bay one-storey RC infilled frame in a non-linear incremental framework. At increasing seismic excitation level, accounting for infills' capacity degradation due to IP/OOP interaction seems to be unavoidable in order to estimate correctly the expected displacement demand.

In future works, the proposed model can be used for structural analyses on multi-storey structures in order to evaluate the effects of the IP/OOP interaction in terms of structural and non-structural elements response as well as to compare the observed OOP demand on infills with the predictions of code provisions. Generally speaking, several issues deserve future dedicated studies. Dynamic shaking table tests aimed at validating the proposed model should be performed. Moreover, a deeper knowledge should be achieved on the effects of the OOP action on the infills IP behaviour, the OOP ultimate displacement reduction due to the IP action, the damping associated to infills OOP behaviour. Experimental pseudo-static and dynamic tests, analytical investigations and modelling efforts should be carried out on such issues.

9 NOTATION

List of symbols

w	infill width	f'_m	masonry compressive strength	**subscripts**	
h	infill height	τ_{cr}	masonry shear strength	m	masonry
t	infill thickness	E	elastic modulus	c	column
h/t	infill slenderness	G	shear modulus	b	beam

ACKNOWLEDGEMENTS

This work was developed under the financial support of METROPOLIS (*Metodologie e tecnologie integrate e sostenibili per l'adattamento e la sicurezza di sistemi urbani - PON Ricerca e Competitività 2007-2013*) and *ReLUIS-DPC 2014-2018 Linea Speciale RS12 Tamponature*, funded by the Italian Department of Civil Protection (DPC). These supports are gratefully acknowledged.

REFERENCES

[1] A. Penna, P. Morandi, M. Rota., Performance of masonry buildings during the Emilia 2012 earthquake. *Bulletin of Earthquake Engineering*, **12.5**, 2255-2273, 2014. DOI:10.1007/s10518-013-9496-6

[2] F. Braga, V. Manfredi, A. Masi et al., Performance of non-structural elements in RC buildings during the L'Aquila, 2009 earthquake. *Bulletin of Earthquake Engineering* **9.1**, 307-324, 2011. DOI:10.1007/s10518-010-9205-7

[3] R.S. Vicente, H. Rodrigues, H. Varum et al., Performance of masonry enclosure walls: lessons learned from recent earthquakes. *Earthquake engineering and engineering vibration,* **11.1**, 23-34, 2012.

[4] P. Ricci, F. De Luca, G.M. Verderame, 6th April 2009 L'Aquila earthquake, Italy: reinforced concrete building performance. *Bulletin of Earthquake Engineering*, **9.1**, 285-305, 2011.

[5] S. Taghavi, E. Miranda, Seismic performance and loss assessment of nonstructural building components. *Proceedings of 7th National Conference on Earthquake Engineering*, Boston, United Stated of America, July 21-25, 2002.

[6] M.N. Fardis, T.B. Panagiotakos, Seismic design and response of bare and masonry-infilled reinforced concrete buildings. Part II: infilled structures. *Journal of Earthquake Engineering*, **1.3,** 475-503, 1997.

[7] T.B. Panagiotakos, M.N. Fardis, Seismic response of infilled RC frames structures. *11th World Conference on Earthquake Engineering*, Acapulco, Mexico, June 23-28, 1996.

[8] A. Saneinejad, B. Hobbs, Inelastic design of infilled frames. *Journal of Structural Engineering*, **121.4**, 634-650, 1995.

[9] R.J. Mainstone, On the stiffness and strength of infilled frames. *Proc., Supplement (IV), Paper 7360S, Instn. of Civ. Engrs.*, London, England, 1971.

[10] R.D. Flanagan, R.M. Bennett, In-plane behaviour of structural clay tile infilled frames. *Journal of Structural Engineering*, **125.6**, 590-599, 1999.

[11] M. Pasca, L. Liberatore, Predicting models for the evaluation of out-of-plane ultimate load carrying capacity of masonry infill walls. *WIT Transactions on the Built Environment*, **152**, 83-94, 2015.

[12] S.P. Timoshenko, S. Woinowsky Krieger, *Theory of plates and shells*. McGraw-Hill, New York, 1959.

[13] E.L. McDowell, K.E. McKee, E. Sevin, Arching action theory of masonry walls. *Journal of the Stuctural Division*, **82.2**, 1-8, 1956.

[14] R. Angel, D.P. Abrams, D. Shapiro et al., *Behaviour of reinforced concrete frames with masonry infills*. University of Illinois Engineering Experiment Station. College of Engineering. University of Illinois at Urbana-Champaign., 1994.

[15] J.L. Dawe, C.K. Seah, Out-of-plane resistance of concrete masonry infilled panels. *Canadian Journal of Civil Engineering*, **16.6**, 854–864, 1989.

[16] R.E. Klinger, N.R. Rubiano, T. Bashandy, Evaluation and analytical verification of shaking table data from infilled frames. *The Masonry Society Journal*, **15.2**, 33-41, 1997.

[17] D.P. Abrams, R. Angel, J. Uzarski, Transverse strength of damaged URM infills. *The professional Journal of the Masonry Society*, **12.1**, 45-52, 1993.

[18] R.D. Flanagan, R.M. Bennett, Arching of masonry infilled frames: Comparison of analytical methods. *Practice Periodical on Structural Design and Construction*, **4.3**, 105-110, 1999.

[19] S. Kadysiewski, K.M. Mosalam, *Modelling of unreinforced masonry infill walls considering in-plane and out-of-plane interaction*. Pacific Earthquake Engineering Research Center, 2009.

[20] R.D. Blevins, *Formulas for natural frequency and mode shape*. Van Nostrand Reinhold Company, Inc., 1979.

[21] M.C. Griffith, J. Vaculik, N.T.K. Lam et al., Cyclic testing of unreinforced masonry walls in two-way bending. *Earthquake Engineering & Structural Dynamics*, **36.6**, 801-821, 2007.

[22] I. Sharif, C.S. Meisl, K.J. Elwood, Assessment of ASCE 41 height-to-thickness ratio limits for URM walls. *Earthquake Spectra*, **23.4**, 893-908, 2007.

[23] ATC, 1997a, NEHRP Guidelines for the Seismic Rehabilitation of Buildings, prepared by the Applied Technology Council (ATC-33 project) for the Building Seismic Safety

Council, published by the Federal Emergency Management Agency, Report No. FEMA273, Washington, D.C.

[24] ATC, 1997b, NEHRP Commentary on the Guidelines for the Seismic Rehabilitation of Buildings, prepared by the Applied Technology Council (ATC-33 project) for the Building Seismic Safety Council, published by the Federal Emergency Management Agency, Report No. FEMA274, Washington, D.C.

[25] ATC, 1998a, Evaluation of Earthquake Damaged Concrete and Masonry Wall Buildings, Basic Procedures Manual, prepared by the Applied Technology Council (ATC-33 project) for the Partnership for Response and Recovery, published by the Federal Emergency Management Agency, Report No. FEMA306, Washington, D.C.

[26] NZSEE Assessment and improvement of the structural performance of buildings in earthquake. Recommendations of a NZSEE Study Group, New Zealand Society for Earthquake Engineering, Wellington, New Zealand, 2006.

[27] EN 1996-1-1 Eurocode 6: Design of masonry structures - Part 1-1: General rules for reinforced and unreinforced masonry structures, 2005.

[28] FEMA 356. Prestandard and commentary for the seismic rehabilitation of buildings. Washington, DC: Federal Emergency Management Agency, 2000.

[29] M.C. Griffith, J. Vaculik, Out-of-plane flexural strength of unreinforced clay brick masonry walls. *The Masonry Society Journal*, **25.1**, 53-68, 2007.

[30] R.D. Flanagan, R.M. Bennett, Bidirectional behaviour of structural clay tile infilled frames. *Journal of Structural Engineering*, **125.3**, 236-244, 1999.

[31] R.D. Flanagan, *Behaviour of structural clay tile infilled frames*. Oak Ridge National Lab., TN (United States), 1994.

[32] G.M. Calvi, D. Bolognini, Seismic response of reinforced concrete frames infilled with weakly reinforced masonry panels. *Journal of Earthquake Engineering*, **5.2**, 153-185, 2001.

[33] M.F.P. Pereira, M.F. Pereira, J.E. Ferreira et al., Behaviour of masonry infill panels in RC frames subjected to in plane and out of plane loads. *7th International Conference on Analytical Models and New Concepts in Concrete and Masonry Structures*, Kraków, Poland, June 13-15, 2011.

[34] G. Guidi, F. da Porto, M. Dalla Benetta et al., Comportamento sperimentale nel piano e fuori piano di tamponamenti in muratura armata e rinforzata. *Proceedings of the XV ANIDIS, L'Ingegneria Sismica in Italia*, Padua, Italy, June 30 – July 4, 2013 (in Italian).

[35] A. Furtado, H. Rodrigues, A. Arêde, H. Varum, Experimental Characterization of the In-plane and Out-of-Plane Behaviour of Infill Masonry Walls. *Procedia Engineering*, **114**, 862-869, 2015. DOI:10.1016/j.proeng.2015.08.041.

[36] A. Furtado, H. Rodrigues, A. Arêde, H. Varum, Experimental evaluation of out-of-plane capacity of masonry infill walls. *Engineering Structures*, **111**, 48-63, 2016.

[37] S. Hak, P. Morandi, G. Magenes, Out-of-plane experimental response of strong masonry infills. *2nd European Conference on Earthquake Engineering and Seismology*, Istanbul, Turkey, August 24-29, 2014.

[38] N.R. Draper, H. Smith, *Applied Regression Analysis*, *3rd Edition*. John Wiley & Sons, Inc. New York, 1998.

[39] M.N. Fardis (editor), *Experimental and numerical investigations on the seismic response of RC infilled frames and recommendations for code provisions, ECOEST/PREC8 Report No.6*, Laboratorio Nacional de Engenharia Civil Publications, Lisbon, 1996.

[40] G. Al-Chaar, *Evaluating strength and stiffness of unreinforced masonry infill structures*. Engineer research and development center Champaign (IL) Construction Engineering Research Lab, 2002.

[41] S.A. Hashemi, K.M. Mosalam, *Seismic evaluation of reinforced concrete buildings including effects of infill masonry walls*. Pacific Earthquake Engineering Research Center, 2007.

[42] A. Furtado, H. Rodrigues, A. Arede, H. Varum, Simplified macro-model for infill masonry walls considering the out-of-plane behaviour. *Earthquake Engineering & Structural Dynamics*, **45.4**, 507-524, 2015. DOI: 10.1002/eqe.2663.

[43] F. Longo, G. Granello, G. Tecchio, F. da Porto, C. Modena, A masonry infill wall model with in-plane out-of-plane interaction applied to pushover analysis of RC frames. *Brick and Block Masonry: Proceedings of the 16th International Brick and Block Masonry Conference*, Padua, Italy, June 26-30, 2016.

[44] P.B. Shing, L. Cavaleri, F. Di Trapani, Prediction of the out-of-plane response of infilled frames under seismic loads by a new fiber-section macro-model. *Brick and Block Masonry: Proceedings of the 16th International Brick and Block Masonry Conference*, Padua, Italy, June 26-30, 2016.

[45] M. Oliaee, G. Magenes, In-plane out-of-plane interaction in the seismic response of masonry infills in RC frames. *Brick and Block Masonry: Proceedings of the 16th International Brick and Block Masonry Conference*, Padua, Italy, June 26-30, 2016.

[46] F. McKenna, G.L. Fenves, M.H. Scott, *Open system for earthquake engineering simulation*. University of California, Berkeley, CA, 2000.

[47] D. Vamvatsikos, C.A. Cornell, Incremental dynamic analysis. *Earthquake Engineering and Structural Dynamics*, **31.3**, 491-514, 2002.

[48] Eurocode 2 (ENV 1992-1-1). Design of concrete structures. 1: General rules and rules for buildings, Brussels, 2004.

[49] Eurocode 8 (1998-3). Design provisions for earthquake resistance of structures. Brussels, Belgium: European Committee for Standardization, 2003.

[50] Federal Emergency Management Agency. Quantification of building seismic performance factors. Applied Technology Council ATC-63 Project Report, FEMA P695, Washington DC, USA, 2009.